Supplemental Document

Biomedical Optics EXPRESS

Noninvasive assessment of liver function reserve with fluorescent dosimetry of indocyanine green: supplement

Pei-Chun Wu,[1,2,3,14] Lun-Zhang Guo,[2,14] Shan Yu,[1,4,14] Ning Zeng,[5,6,14] Yu-Cheng Liu,[1] Jia Yu,[1] Zhiming Zhang,[1] Ke Lu,[1] Liangyu Sun,[1] Chunfei Wang,[1] Yu-Han Chang,[2,3] Yin-Lin Lu,[1,3] Yu-Fang Shen,[7,8] Sheng Tai,[9] Yueh-Hsun Chuang,[10] Ja-An Annie Ho,[11] Kai-Wen Huang,[12] Yao-Ming Wu,[13] and Tzu-Ming Liu[1,*]

[1] *Institute of Translational Medicine, Faculty of Health Sciences & Ministry of Education Frontiers Science Center for Precision Oncology, University of Macau, Taipa, Macau, China*
[2] *Department of Biomedical Engineering, National Taiwan University, Taipei 10617, Taiwan*
[3] *Molecular Imaging Center, National Taiwan University, Taipei 10617, Taiwan*
[4] *Department of Pathology, The Secondary Affiliated Hospital of Harbin Medical University, Harbin 150080, China*
[5] *First Department of Hepatobiliary Surgery, Zhujiang Hospital, Southern Medical University, Guangzhou 510280, China*
[6] *Guangdong Provincial Clinical and Engineering Technology Center of Digital Medicine, Guangzhou 510280, China*
[7] *3D Printing Medical Research Institute, Asia University, Taichung 41354, Taiwan*
[8] *Department of Bioinformatics and Medical Engineering, Asia University, Taichung 41354, Taiwan*
[9] *Department of Hepatopancreatobiliary Surgery, The Secondary Affiliated Hospital of Harbin Medical University, Harbin 150080, China*
[10] *Department of Anesthesiology, National Taiwan University Hospital, Taipei 10002, Taiwan*
[11] *Bioanalytical Chemistry and Nanobiomedicine Laboratory, Department of Biochemical Science & Technology, National Taiwan University, Taipei 10617, Taiwan*
[12] *Graduate Institute of Clinical Medicine, National Taiwan University College of Medicine, Taipei 10002, Taiwan*
[13] *Department of Surgery, National Taiwan University Hospital and College of Medicine, Taipei 10002, Taiwan*
[14] *Contributed equally*
[*] *tmliu@um.edu.mo*

Supplement DOI: https://doi.org/10.6084/m9.figshare.19173923

Parent Article DOI: https://doi.org/10.1364/BOE.446749

Noninvasive Assessment of Liver Function Reserve with Fluorescent Dosimetry of Indocyanine Green

Table S1. Quantification of serum biomarkers related to the liver function of rats

	Control Group	Rat 1	Rat 2	Rat 3
Albumin (g/dL)	4.1	3.9	4	3.75
Total bilirubin(mg/dL)	0.4	0.27	0.4	0.6
GPT（U/L）	58.5	60.3	96	129
GOT（U/L）	85.5	89	247	265

Table S2. Fitting parameters of curves in Fig. 3(b) and 3(c).

	Y-axis intercept y_0	Amplitude A	Decay time τ (minute)
Control	0	99.967	4.460
Rat 1	5.959	94.093	3.816
Rat 2	1.078	98.920	4.452
Rat 3	1.716	98.193	13.898

Table S3. Fitting parameters of curves in Fig. 4.

	Y-axis intercept y_0	Amplitude A	Decay time τ (minute)
1×(black curve)	0.020	0.980	4.645
1×(red curve)	0.011	0.986	4.554
0.1×(black curve)	0.000	0.999	4.973
0.1×(red curve)	0.000	1.000	4.438
0.1×(blue curve)	0.010	0.990	4.865

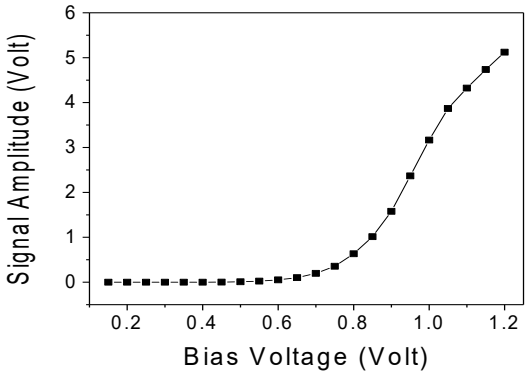

Fig. S1. Bias-dependent background signals of PBS buffer. The excitation power of the 785 nm laser was 50 mW.

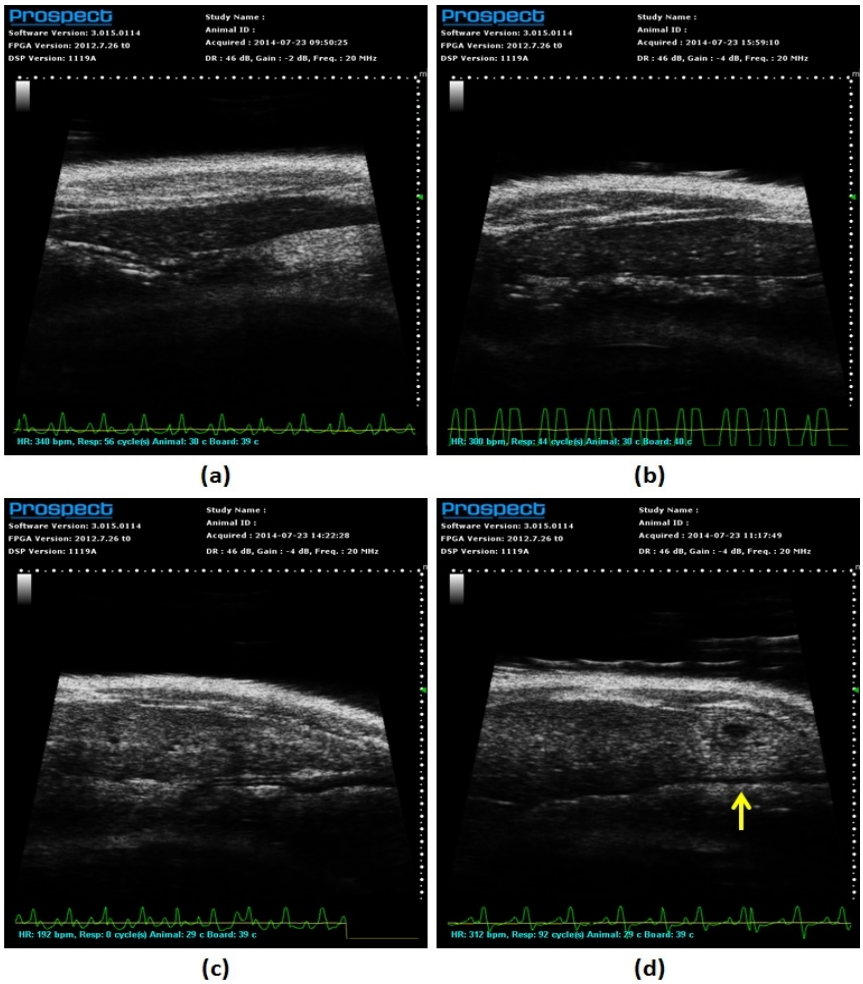

Fig. S2. High-frequency ultrasound images of livers in (a) Control rat (b) Rat 1 (c) Rat 2 (d) Rat 3. The yellow arrow indicates the tumor area.

Liver Lesion Confirmed by H&E and Masson Staining

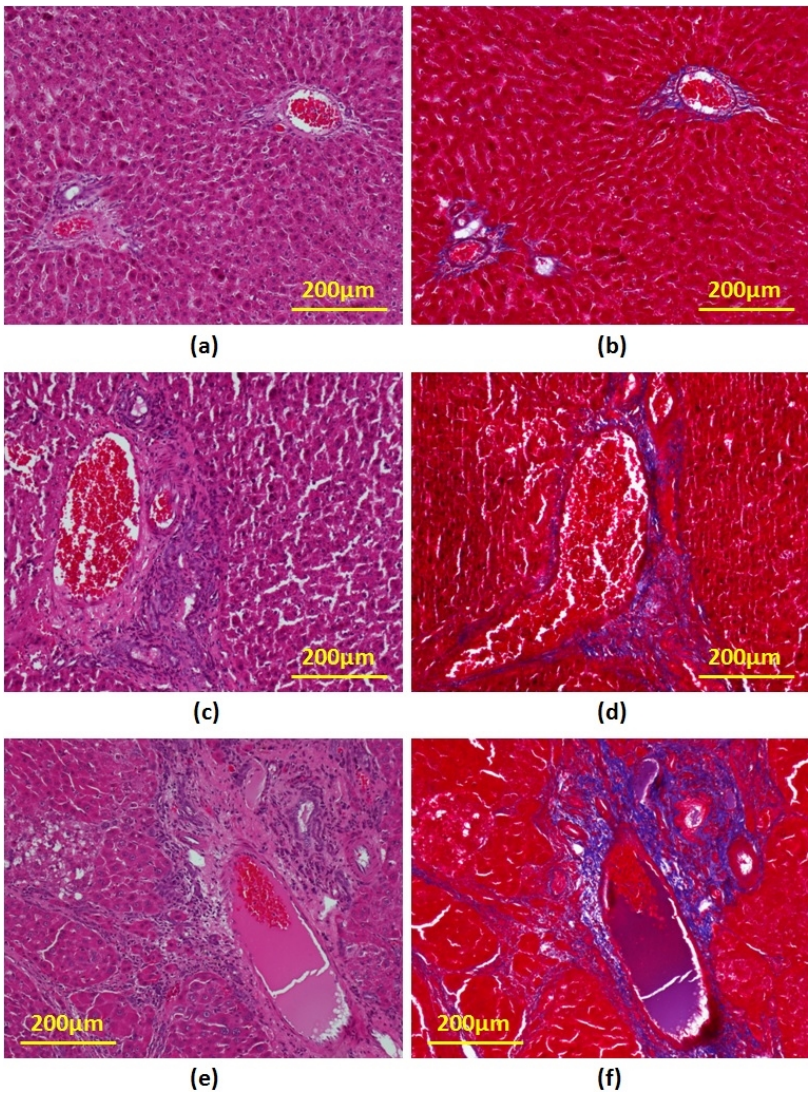

Fig. S3. A representative comparison of the portal zone in different groups. (a,b) Control, (c,d) Rat 1, (e,f) Rat 3. (a.c.e) H&E staining; (b,d,f) Masson Staining.

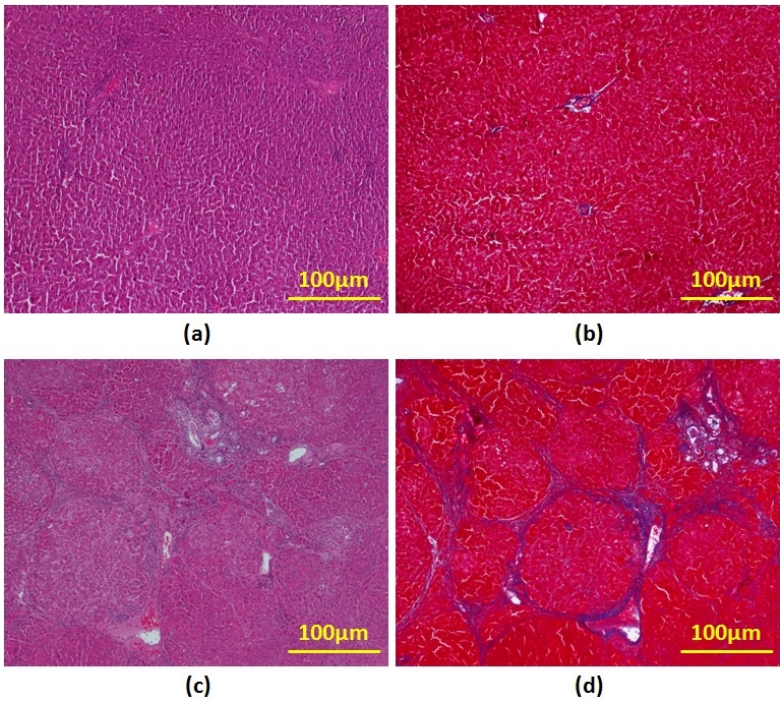

Fig. S4. Representative liver staining pictures. (a,c) H&E staining; (b,d) Masson staining. (a,b) Rat 1 shows no significant lesion in the liver. (c,d) Rat 3 shows architectural distortion (septal fibrosis, bridging) and pseudolobules formation.

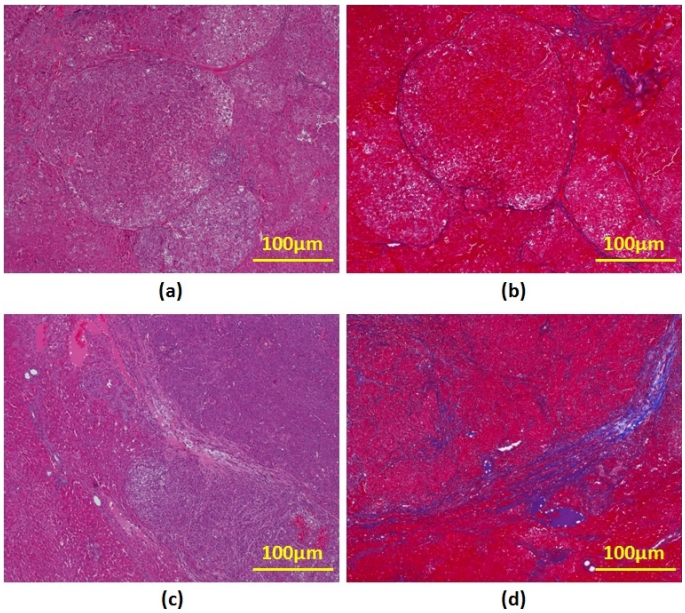

Fig. S5. Rat 2's liver sections. (a,b) H&E and Masson staining show that the tumor region lacks collagen structure and fibrous septa separating thick plates (c,d) Non-tumor region shows regenerated hepatocytes with a dark purple in H&E staining. Masson staining pattern is different from cirrhosis area, but fibrosis is widely present.

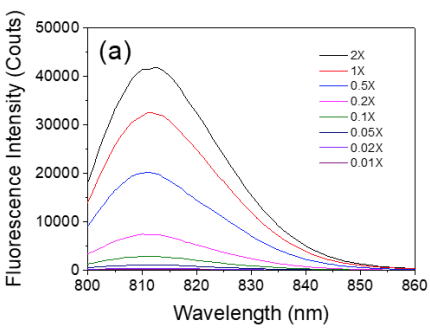

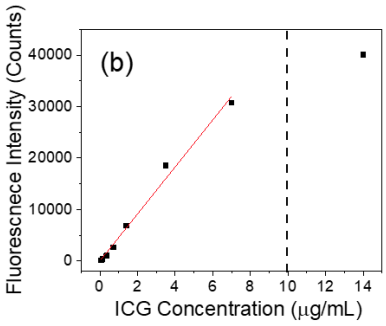

Equation	y = a + b*x
Plot	B
Weight	No Weighting
Intercept	36.8565 ?640.32936
Slope	4565.31189 ?212.02
Residual Sum of Squa	8.78982E6
Pearson's r	0.99465
R-Square(COD)	0.98933
Adj. R-Square	0.9872

Fig. S6. (a) Single-photon fluorescence spectrum of ICG at different clinical dosages. (λ_{ex}=785 nm, 1× dosage = 12.7 μg/mL); (b) The ICG fluorescence intensities at various concentrations. The 14 μg/mL already showed saturation effect and was not included in the data's linear fitting (red line). The table below shows the fitting results.

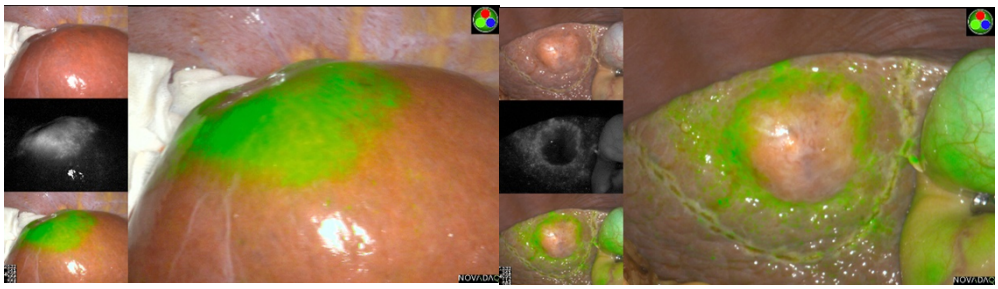

Fig. S7. The bright-field color images (top), ICG fluorescence images (middle), and combined images (bottom, green color represent ICG) of human HCC tissues (enlarged view to the right). After ICG-R15 testing, the well-differentiated HCC (Left image set) showed a cholestasis-like accumulation, while the poor-differentiated HCC (Right) showed a ring around the tumor site.